Research Article **Open Access**

Marta Ferraroni[#], Adrie H. Westphal[#], Marco Borsari[#], Juan Antonio Tamayo-Ramos, Fabrizio Briganti[†], Leo H. de Graaff[†], Willem J. H. van Berkel*

Structure and function of *Aspergillus niger* laccase McoG

DOI 10.1515/boca-2017-0001
Received October 10, 2016; accepted December 8, 2016

Abstract: The ascomycete *Aspergillus niger* produces several multicopper oxidases, but their biocatalytic properties remain largely unknown. Elucidation of the crystal structure of *A. niger* laccase McoG at 1.7 Å resolution revealed that the C-terminal tail of this glycoprotein blocks the T3 solvent channel and that a peroxide ion bridges the two T3 copper atoms. Remarkably, McoG contains a histidine (His253) instead of the common aspartate or glutamate expected to be involved in catalytic proton transfer with phenolic compounds. The crystal structure of H253D at 1.5 Å resolution resembles the wild type structure. McoG and the H253D, H253A and H253N variants have similar activities with 2,2'-azino-bis(3-ethylbenzothiazoline-6-sulphonic acid or *N,N*-dimethyl-*p*-phenylenediamine sulphate. However, the activities of H253A and H253N with 2-amino-4-methylphenol and 2-amino-4-methoxyphenol are strongly reduced compared to that of wild type. The redox potentials and electron transfer rates (k_s) of wild type and variants were determined (McoG wt E°' is +453 mV), and especially the reduced k_s values of H253A and H253N show strong correlation with their low activity on phenolic compounds. In summary, our results suggest that the His253 adaptation of McoG can be beneficial for the conversion of phenolic compounds.

Keywords: *Aspergillus niger*; crystal structure; laccase; redox potential; metalloprotein; multicopper oxidase

Data deposition: Coordinates have been deposited with the Protein Data Bank. Accession codes are 5LM8, 5LWW and 5LWX.

Abbreviations: CV, cyclic voltammetry; DT, decane-1-thiol; MCO, multicopper oxidase; *Ma*L, laccase from *Melanocarpus albomyces*; *Ta*L, laccase from *Thielavia arenaria*; SAM, self-assembled monolayer; SCE, saturated calomel electrode; SHE, standard hydrogen electrode; DMPPDA, *N,N*-dimethyl-*p*-phenylenediamine; ABTS, 2,2'-azino-bis(3-ethylbenzothiazoline-6-sulphonic acid).

1 Introduction

Multicopper oxidases (MCOs) form a family of redox enzymes that catalyze the reduction of molecular oxygen into water by a four-electron transfer process. It includes laccases (EC 1.10.3.2), ascorbate oxidases (EC 1.10.3.3), bilirubin oxidases (EC 1.3.3.5) and ferroxidases (EC 1.16.3.1), which are key enzymes in many biological processes of prokaryotic and eukaryotic organisms [1, 2]. Their ability to catalyze the oxidation of various aromatic substrates with the concomitant reduction of molecular oxygen to water as sole byproduct makes them interesting green biocatalysts. The MCO catalyzed redox process is mediated by two copper centers, which contain

***Corresponding author: Willem J. H. van Berkel**, Laboratory of Biochemistry, Wageningen University & Research, Stippeneng 4, Wageningen 6708 WE, The Netherlands,
E-mail: willem.vanberkel@wur.nl
Marta Ferraroni, Fabrizio Briganti, Department of Chemistry 'Ugo Schiff', University of Florence, Via della Lastruccia 3, I-50019 Sesto Fiorentino, Italy
Adrie H. Westphal, Laboratory of Biochemistry, Wageningen University & Research, Stippeneng 4, Wageningen 6708 WE, The Netherlands
Marco Borsari, Department of Chemical and Geological Sciences, University of Modena and Reggio Emilia, Via Campi 103, I-41125 Modena, Italy
Juan Antonio Tamayo-Ramos, Leo H. de Graaff, Microbial Systems Biology, Laboratory of Systems and Synthetic Biology, Wageningen University & Research, Stippeneng 4, Wageningen 6708 WE, The Netherlands
Juan Antonio Tamayo-Ramos, International Research Center in Critical Raw Materials for Advanced Industrial Technologies (ICCRAM), University of Burgos, Plaza Misael Bañuelos s/n, 09001, Burgos, Spain
[#]Authors contributed equally
[†]Prof. Dr. Fabrizio Briganti passed away on 22 June 2012.
We dedicate this article to Dr. Leo H. de Graaff, who passed away on 6 October 2016.

in total four copper atoms, classified as T1 (one copper), T2 (one copper), and T3 (two coppers) according to their spectroscopic characteristics [3]. Laccases form the largest subgroup within the MCO family and have received most of the attention in biochemical and biotechnological studies [2, 4]. They are generally extracellular monomeric glycoproteins with molecular weights ranging from 60 to 80 kDa, and up to 30% of their molecular weight can be made up of carbohydrates [4]. These enzymes are widely distributed in nature and in fungi, laccase activities have been related to the degradation of lignocellulose material, the production of pigments, processes of morphogenesis, sporulation, the involvement in pathogenesis toward plants and animals [5] and the oxidation of antibiotics produced by microorganisms [6]. In addition, laccases can oxidize non-phenolic compounds through the inclusion of redox mediators, with which they are able to oxidize e.g. lignin, cellulose or starch [7]. This ability is used in various biotechnological processes, including the breakdown of colorants, bioremediation, biopulping and the synthesis of pharmaceutical products [8]. Laccases are present in various groups of fungi, including yeasts [9], filamentous ascomycetes [10] and white [11] and brown rot fungi [12], as well as mycorrhizal species [13]. In particular, basidiomycete laccases of several *Trametes* and *Pleurotus* species have been well characterized. *Aspergillus* MCOs, included in the ascomycete laccases cluster, have received little attention. A significant number of these enzymes, including *A. nidulans* LccA, LccB and LccC [14] and the MCO group from *A. niger* remain largely uncharacterized [15]. Interestingly, *A. niger* MCOs have a low similarity to laccases present in the basidiomycete laccases cluster (around 25% identical). Thus, to obtain insight into the biological role and possible biotechnological potential of this particular group of MCOs, more knowledge about their structure and function is required. Recently, ten of these *A. niger* laccases were homologously overexpressed, revealing remarkable biochemical differences [10]. Here, we address the structural and catalytic properties of one of these, McoG, which has an unusual histidine (His253) in the active site, and in addition, the properties of three variants (H253D, H253A and H253N).

2 Material and methods

2.1 Chemicals

Pfu DNA polymerase, DpnI and dNTPs were purchased from Invitrogen (Carlsbad, CA, USA). Oligonucleotides were synthesized by Eurogentec (Liege, Belgium). QuikChange Lightning Site-Directed Mutagenesis Kit was from Agilent Technologies, Amstelveen, The Netherlands. Aromatic compounds were purchased from Sigma-Aldrich Chemie B.V. (Zwijndrecht, The Netherlands) and Acros Organics (Geel, Belgium). Deglycosylation kit EndoHf was from New England Biolabs GMBH, (Frankfurt am Main, Germany). The JCSG-plusTM Screen used was from Molecular Dimensions Ltd (Suffolk, UK). Other crystallization kits were purchased from New Hampton (Aliso Viejo, CA, USA). 30 kDa cutoff ultrafiltration filters were from Millipore (Merck Chemicals B.V., Amsterdam, The Netherlands). BCA assay kit was from Thermo Scientific (Ulm, Germany). All other chemicals were from commercial sources and of the purest grade available.

2.2 Molecular biology techniques and transformation

Escherichia coli strain DH5α [endA1, hsdR17, gyrA96, thi-1, relA1, supE44, recA1, ΔlacU169 (Φ80 lacZΔM15)] was used as a recipient strain for plasmid transformation and amplification. Standard methods were used to carry out DNA manipulations [16]. Genomic DNA was isolated from *A. niger* N593 as described previously [17]. Mutations in the McoG gene, His253Ala (H253A), His253Asp (H253D), and His253Asn (H253N), were introduced by PCR reactions using the QuikChange Lightning Site-Directed Mutagenesis Kit according to the manufacturer's instructions. The plasmid pGWmcoG [10], expressing *mcoG* under the control of the *glaA* promoter, and carrying the selection marker *pyrA*, was used as DNA template. The following primers were used to introduce the point mutations:
JAT_mcoG253Asp_for:
tggtcaatgccgccatggatacccattttaggttc,
JAT_mcoG253Asp_for_antisense:
gaacctaaaatgggtatccatggcggcattgacca,
JAT_mcoG253Asn_for:
tggtcaatgccgccatgaatacccattttaggttc,
JAT_mcoG253Asn_for_antisense:
gaacctaaaatgggtattcatggcggcattgacca,
JAT_mcoG253Ala_for:
gttggtcaatgccgccatggctacccattttaggttctca,
JAT_mcoG253Ala_for_antisense:
tgagaacctaaaatgggtagccatggcggcattgaccaac.

Fungal transformations were made using the *pyrA* deficient strain *A. niger* N593 for the homologous expression of the different McoG versions, using a similar protocol to the one described in Oliveira et al. [18]. In brief, enzymatic degradation of fungal cell wall was used to generate

protoplasts, followed by purification by filtration and storage in isotonic sorbitol solution. For PEG-mediated transformations, four protoplast aliquots were incubated with 10 µg of the various pGWmcoG plasmid versions (wild type and three mutants). After this procedure, protoplasts were dispersed in sucrose-stabilized minimal medium agar (0.6% (w/v) agar, 0.95 M sucrose, pH 6.0), which was layered on sucrose-stabilized minimal medium agar plates (1.2% (w/v) agar, 0.95 M sucrose, pH 6.0). Plates were incubated 4 days at 30°C. After this period, spores were transferred from each strain to individual minimal medium agar plates containing 50 mM glucose and supplements.

2.3 Sequence alignment

The amino acids sequences for McoG from *Aspergillus niger* (5LM8) and for the laccases from *Botrytis aclada* (3SQR), *Melanocarpus albomyces* (1GW0), *Thielavia arenaria* (3PPS), *Trametes* sp. AH28-2 (3KW7), *Antrodiella faginea* (5EHF), *Coriolopsis caperata* (4JHU), *Coriolopsis gallica* (5A7E) and *Steccherinum murashkinskyi* (5E9N) were aligned using the PROMALS3D server [19], which also uses structural information in constructing the alignment. The figure showing the alignment was made using ESpript server [20].

2.4 *Aspergillus niger* cultivation and laccase production

A. niger N593 strain was used as a host for expression genes coding for the wild-type protein McoG, and for variants H253A, H253D, and H253N. Complete medium agar plates were used for preparation of spores [21, 22]. After 5 days of incubation at 30°C, spores were harvested using a 1% saline solution. Liquid cultures (800 mL of minimal medium, inoculated with around $1*10^6$ spores) were grown in 2 L Erlenmeyer flasks placed in an orbital shaker (250 rpm) for 24 h at 30°C. Minimal medium contained 0.5 g/L KH_2PO_4, 0.5 g/L KCl, 0.5 g/L $MgSO_4 \bullet 7H_2O$, 0.1% yeast extract, 0.5% Casamino acids, 2 g/L of maltose, 13.5 g/L ammonium tartrate, 1 mL Vishniac trace-elements solution and 32 mg/L of Cu_2SO_4 [22]. A clear solution was obtained from 1.6 L of culture by filtration through a nylon mesh. The solution was brought to pH 6.5 and next diluted with demi water to 7.5 L. Sedimented Streamline Q XL agarose beads (GE Healthcare) (20 mL) were added to the diluted solution and gently stirred overnight at 4°C. The next day, beads were allowed to settle for 1 hr. Subsequently, the solution was carefully decanted and the beads collected. The efficiency of binding of McoG was tested by activity measurements of samples taken before and after the incubation with the Streamline Q material and was typically found to be around 95 percent [15].

2.5 Enzyme Purification

The Streamline Q XL agarose beads containing bound McoG protein were washed three times with 40 mL 20 mM Tris-HCl, pH 7.5 and subsequently poured into a small column. The McoG was eluted from the beads using a 400 mL gradient from 0 - 1 M NaCl in 20 mM Tris-Cl, pH 7.5. Active fractions were pooled and concentrated using a 30 kDa cutoff ultrafiltration filter. The concentrated protein solution was loaded on a Superdex 200 column (25 by 600 mm) and eluted with 20 mM Tris-Cl, 150 mM NaCl, pH 7.5. This step separated the protein, especially from relatively low mass yellowish compounds excreted by the fungus. The fractions containing the pure McoG protein, as judged from SDS-polyacrylamide gels, were pooled, concentrated, flash-frozen in liquid nitrogen and stored at -80°C. To check the quality and purity of the obtained McoG proteins, 8 % discontinuous Tricine SDS-polyacrylamide gels were run. Staining was performed with Coomassie Brilliant Blue (Bio-Rad). For protein quantification, a BCA assay was used with bovine serum albumin as standard. Deglycosylation of wild-type McoG and H253D, H253A and H253N variants was performed using an $EndoH_f$ kit (Endoglycosidase H) according to the manufacturer's protocol.

2.6 Enzyme activity measurements

The activities of McoG and the His253 variants with 2,2'-azino-bis(3-ethylbenzothiazoline-6-sulphonic acid) (ABTS) and *N,N*-dimethyl-*p*-phenylenediamine sulphate (DMPPDA) were determined by following the absorbance change caused by changing substrate or formed product concentration in time using a spectrophotometer with a thermostatted cuvette holder at 25°C (Ultrospec 2000, Pharmacia Biotech), coupled to a recorder unit. Substrates were dissolved, if necessary, in DMSO, and diluted to the desired end-concentration in 100 mM sodium acetate buffer, pH 6.0, in a total volume of 1 mL. Care was taken to keep the amount of DMSO constant and below 5% in the assay mixture. Catalytic amounts of McoG were quickly mixed into this solution and absorption change rates measured. Molar absorption coefficients used are for ABTS: $\varepsilon_{414} = 36800\ M^{-1}cm^{-1}$ and for DMPPDA: $\varepsilon_{550} = 7500\ M^{-1}cm^{-1}$.

The activities of McoG and the His253 variants with 2-amino-4-methylphenol and 2-amino-4-methoxyphenol

were determined from oxygen consumption experiments. Oxygraph measurements were performed at 25°C using a stirred Clark-type electrode (Hansatech Oxytherm system, Wittich & Visser, Rijswijk, The Netherlands). Substrates were dissolved, if necessary, in DMSO, and diluted to the desired end-concentration in 100 mM sodium acetate buffer pH 6.0 in a total volume of 1 mL. Care was taken to keep the amount of DMSO constant and below 5% in the assay mixture. Catalytic amounts of McoG were added to this solution using a Hamilton syringe and oxygen decrease rates measured.

To test the influence of additional metal ions on the activity of McoG wt using ABTS as substrate, 25 mM $ZnCl_2$ or $CuCl_2$ was added to the assay mixture.

Electrochemistry

Cyclic voltammetry (CV) experiments were performed with a PAR model 273A potentiostat/galvanostat (Princeton Applied Research, Oak Ridge, USA) at different scan rates (0.02-2 Vs^{-1}), using a three-electrode cell for small volume samples (0.5 mL) under argon. A polycrystalline gold wire (diameter 1 mm) was used as working electrode, and a platinum sheet electrode and a saturated calomel electrode (SCE) were used as counter and reference electrodes, respectively. A Vycor glass frit set (PAR) ensured the electric contact between the SCE and the working solution. Formal (reduction) potential values (E°') are calculated as $E°' = (E_{pa}+E_{pc})/2$, where E_{pa} and E_{pc} are the anodic and cathodic peak potentials, respectively, and are referenced to the standard hydrogen electrode (SHE). Prior to use, the gold working electrode was submersed in concentrated nitric acid for 10 min, flamed under oxidizing conditions and heated in 2.5 M KOH for 4 hr and, after rinsing in water, soaked in concentrated sulfuric acid for 12 hrs. To minimize residual adsorbed impurities, the electrode was subjected to 15 voltammetric cycles between +0.7 and -0.6 V (vs SCE) at 0.1 V s^{-1} in 1 M H_2SO_4. To generate a self-assembled monolayer (SAM), the cleaned electrode was dipped in 1 mM ethanolic decane-1-thiol (DT) solution for 12 h at 4°C. After rinsing with MilliQ water, the self-assembled monolayer coated electrode (DT-SAM) was subjected to 10 voltammetric cycles from +0.2 V to -0.4 V in a 0.1 M sodium perchlorate solution (outgassed with argon) to align the DT-SAM. The resulting CV was taken as the background and checked for the absence of spurious signals. McoG wt and the variants H253D, H253A and H253N were adsorbed on the alkanethiol-coated gold electrodes by dipping the functionalized electrode into the protein solution (about 120 μM for wt and 140 μM for variants) in 20 mM Tris-Cl, 50 mM NaCl, pH 7.5, at 4°C for 5 hrs. The CV experiments were carried out, using the washed functionalized electrode, using 20 mM Tris-Cl containing 50 mM sodium perchlorate, pH 7.5, as base electrolytes. The experiments were performed at least in triplicate and the *E°'* values were found to be reproducible within ± 2 mV. The surface coverage (Θ = 44, 26, 15 and 13 pmol cm^{-2} for wt, H253D, H253A and H253N, respectively) was calculated from the overall charge exchanged by the protein (determined upon integration of the baseline-corrected anodic or cathodic peaks) and the area of the gold electrode. The latter was determined electrochemically by recording the CV of a standard aqueous solution of ferrocenium tetrafluoborate in a diffusion-controlled regime, in which the bare electrode was dipped at exactly the same depth as for the measurements with adsorbed McoGs.

CVs at variable scan rates (from 0.020 to 1 Vs^{-1}) were recorded to determine the heterogeneous ET rate constant (k_s) for the adsorbed protein using the Laviron method [23]. The k_s values were averaged over five measurements and found to be reproducible (± 6%), which was taken as the error on these measurements.

The thermodynamic parameters $\Delta S°'_{rc}$ and $\Delta H°'_{rc}$ for Cu(II) to Cu(I) reduction (T1 center) were determined from variable-temperature E°' measurements carried out using a "non-isothermal" electrochemical cell, in which the reference electrode is kept at constant temperature ((21.0 ± 0.1)°C) whereas the half-cell containing the working electrode and the Vycor junction is under thermostatic control [24-26]. With this experimental configuration, the reaction entropy for reduction of the oxidized protein ($\Delta S°_{rc}$) is given by equation (1),

$$\Delta S^{0'}_{rc} = S^{0'}_{red} - S^{0'}_{ox} = nF\frac{E^{0'}}{dT} \quad (1)$$

in which *n* is the number of electrons involved in the reaction, *F* is the Faraday constant and *T* is the absolute temperature. $\Delta S°'_{rc}$ was determined using the slope of the plot of E°' versus temperature, which is linear under the assumption that $\Delta S°'_{rc}$ is constant over the temperature range investigated. With the same assumption, the enthalpy change ($\Delta H°'_{rc}$) was derived from the Gibbs-Helmholtz equation and was calculated using equation (2),

$$\Delta H^{0'}_{rc} = -nF\left(E^{0'} - T\frac{dE^{0'}}{dT}\right) \quad (2)$$

in which *n* is the number of electrons involved in the reaction, *F* is the Faraday constant and *T* is the absolute temperature.

The non-isothermal behaviour of the cell was carefully checked by determining the $\Delta H°'_{rc}$ and $\Delta S°'_{rc}$ values of the ferricyanide/ferrocyanide couple [25, 26].

2.7 Protein Crystallization and Data Collection

Concentration of the wild-type protein solution used for the crystallization trials was 20 mg/mL in 20 mM Hepes/NaOH, pH 7.5. The enzyme was crystallized at 296 K using the sitting drop vapor diffusion method in 96-well plates (CrystalQuick, GreinerBio-One, Frickenhausen, Germany) from a solution containing 20% PEG 3000, 0.2 M zinc acetate, 0.1 M imidazole, pH 8.0. Drops were prepared using 1 µL protein solution mixed with 1 µL reservoir solution and were equilibrated against 100 µL precipitant solution. Initial crystallization conditions were found using solutions from the JCSG-plusTM Screen (Molecular Dimensions Ltd, UK). Crystals obtained belong to the primitive orthorhombic space group I222 with unit cell dimensions a=88.45 Å, b=128.16 Å, c=134.68 Å (crystal form I). The asymmetric unit contains one molecule (Vm= 2.94 Å^3/Da, solvent content 58.18%). Before data collection, 10% glycerol of the mother liquor solution was added to a crystal of the enzyme as cryoprotectant. A data set extending to a resolution of 2.65 Å was collected at 100 K on an Oxford Diffraction instrument equipped with a sealed tube Enhance Ultra (Cu) at a wavelength of 1.540 Å and an Onyx CCD detector. Another crystal form was obtained using 20% PEG 3350, 0.2 M NaCl and 0.1 M sodium citrate pH 5.5. Crystals obtained from this solution belong to the monoclinic space group C2 with unit cell dimensions a=200.71 Å, b=61.35 Å, c=53.84 Å and β= 95.30° (crystal form II). The asymmetric unit contains one molecule (Vm= 2.54 Å^3/Da, solvent content 51.56%). A data set extending to a resolution of 1.7 Å was collected at 100 K using the ID29 Beamline of the European Synchrotron Radiation Facility (ESRF, Grenoble, France) at a wavelength of 0.960 Å and a PILATUS 6M detector.

For the McoG variants H253D, H253A and H253N, only H253D yielded good quality crystals. Concentration of H253D used for the crystallization was 17 mg/mL in 20 mM Hepes/NaOH, pH 7.5. The enzyme was crystallized at 296 K using the same crystallization conditions as described above for crystal form II of the wild-type enzyme. A data set extending to 1.5 Å of resolution was collected at 100 K using the BL13-XALOC Beamline of ALBA (Barcelona, Spain) at a wavelength of 0.951 Å and a PILATUS 6M detector. The data sets were processed with XDS [27]. Statistics of the data collection and processing are reported in Table 1.

Table 1. Summary of Data Collection and Atomic Model Refinement Statistics.[1]

	McoG wt Form I	McoG wt Form II	McoG-H253D
Data Collection			
Wavelength (Å)	1.540	0.960	0.951
Space Group	I222	C2	C2
Unit cell (a, b, c, α, β, γ) (Å, °)	88.45, 128.16, 134.68, 90.0, 90.0, 90.0	199.70, 61.35, 53.72, 90.0, 95.04, 90.0	200.27, 60.50, 53.74, 90.0, 94.96, 90.0
Limiting resolution (Å)	29.4-2.65 (2.81-2.65)	30.0-1.7 (1.8-1.7)	29.2-1.5 (1.58-1.49)
Unique reflections	22606 (3554)	65942 (8020)	101840 (15290)
R_{sym} (%)	14.0 (49.8)	6.9 (30.7)	7.4 (98.7)
Multiplicity	3.6 (3.5)	2.6 (2.0)	3.2 (2.6)
Completeness overall (%)	99.7 (99.2)	90.5 (68.5)	98.1 (91.6)
<I/(I)>	14.35 (3.99)	9.11 (2.05)	9.09 (0.97)
Refinement			
Resolution range (Å)	20.0-2.65	30.0-1.7	29.0-1.5
Unique reflections working/free	21395/1154	62765/3292	96750/5091
R-factor (%)	18.48	17.26	17.15
R-free(%)	26.67	22.15	19.57
Non-hydrogen atoms	4738	5179	5171
Water molecules	218	599	497
r.m.s.d. bonds (Å)	0.0133	0.0214	0.0089
r.m.s.d. angles (°)	1.888	2.083	1.307
Average B factor (Å^2)			
All atoms	42.01	29.39	33.82
Protein atoms	42.15	27.40	31.50
Water atoms	37.80	40.16	46.95
PDB ID	5LWW	5LM8	5LWX

[1]Values in parentheses are for the highest resolution shell.

2.8 Structure Determination and Refinement

The McoG structure was solved using the orthorhombic data set (crystal form I) by the Molecular Replacement technique using the program Molrep [28] and the coordinates of laccase from *Melanocarpus albomyces* (PDB code: 1GW0) as a starting model, after deleting all the heteroatoms. (Fo-Fc) electron-density maps, calculated from the Molecular replacement solution after cycles of refinement using Refmac5 [29], showed the presence of glucoside moieties *N*-linked to Asn residues as observed in other laccase structures. Furthermore, numerous spherical densities (typical for metal ions) were located at the enzyme surface. Based on the coordination number and distances, these densities are interpreted as zinc ions, originating from the crystallization medium (see Results and Discussion). Manual rebuilding of the model was performed using the program Coot [30]. Solvent molecules were introduced automatically using ARP [31]. Refinement resulted in R-factor and R-free values of 0.185 and 0.267, respectively. The McoG structure, derived from crystal form II, was solved using Molecular Replacement and the coordinates of the other McoG structure obtained in the presence of zinc. The refinement and model building were performed using the same programs as reported above. Refinement resulted in R-factor and R-free values of 0.173 and 0.221, respectively. Occupancies of the copper ions were adjusted such that their refined B-factors approximated the values of their local environment. In particular, occupancies of the copper ions in the structure obtained from crystal form I were all set to unity, whereas in the structure obtained from crystal form II, occupancies of 0.5 and 0.75 were attributed to CuT3a and CuT2, respectively. The structure of the H253D variant was refined starting from the coordinates of the wild-type McoG structure (form II) and resulted in R-factor and R-free values of 0.172 and 0.196, respectively. The (Fo-Fc) electron-density maps clearly showed the histidine to aspartate substitution at a position corresponding to residue 253. Copper occupancies were set to 1.0 for CuT1 and CuT3b and 0.75 for CuT3a and CuT2. Refinement statistics are summarized in Table 1. The stereochemistries of the final models were analyzed with Coot and Rampage [30, 32]. Protein coordinates have been deposited with the Protein Data Bank (Protein Data Bank accession numbers 5LWW, 5LM8 and 5LWX).

3 Results and Discussion

3.1 Biochemical properties

Thirteen genes coding for laccase-like MCO proteins were identified in the genome of *Aspergillus niger* ATCC 1015 strain, while sixteen were found in *A. niger* CBS 513.88, of which ten were homologously expressed [10]. The McoG coding gene is present in both strains (*A. niger* 1015 protein ID: 1140659; *A. niger* CBS 513.88 protein ID: An08g08450) coding for identical proteins. The *mcoG* gene from *A. niger* N593 strain also codes for the same protein. The genomic DNA of this strain was used as template to PCR-amplify and clone the *mcoG* gene. Usually, in laccases, an aspartate or glutamate residue is found close to the active site, and this residue is believed to be involved in the enzymatic reaction of laccases with phenolic compounds [33, 34]. Figure 1 shows an alignment of the sequence of McoG, one of the MCO proteins from *A. niger*, with eight sequences of laccases with known structure. McoG contains at position 253 a histidine instead of an aspartate or glutamate, as is the case for the other laccases shown. To probe the function of this unusual histidine, we modified it through site-directed mutagenesis into an alanine, aspartate or asparagine residue (H253A, H253D and H253N). Expression and purification of McoG wt and the variants H253A, H253D and H253N yielded ± 40 mg of blue colored proteins from 3 L culture batches. Figure 2 shows a gel image of samples of the four purified proteins after SDS-PAGE. The bands are not very sharp and the apparent masses are too high and also vary between the proteins. *N*-deglycosylation with endoglycosidase H resulted in masses corresponding close to those obtained from their amino acid sequence (65 kDa, Figure S1), indicating that the degree of glycosylation is not identical between the variants, and is also the cause of the aberrant migration on SDS-PAGE.

For a variety of tested compounds, activity was, besides with ABTS and DMPPDA, found highest with 2-amino substituted phenolic substrates, like 2-amino-4-methylphenol and 2-amino-4-methoxyphenol. Activity was low or absent with phenolic compounds containing a carboxylic group. The kinetic parameters K_M and V_{MAX} of wt and His253 variants, determined using absorption changes of DMPPDA and ABTS, and using oxygen consumption with 2-amino-4-methylphenol and 2-amino-4-methoxyphenol, are listed in Table 2. McoG wt has the highest activity with 2-amino-4-methoxyphenol, whereas the H253A variant shows the highest activity with DMPPDA and ABTS. The K_M values for ABTS for all proteins

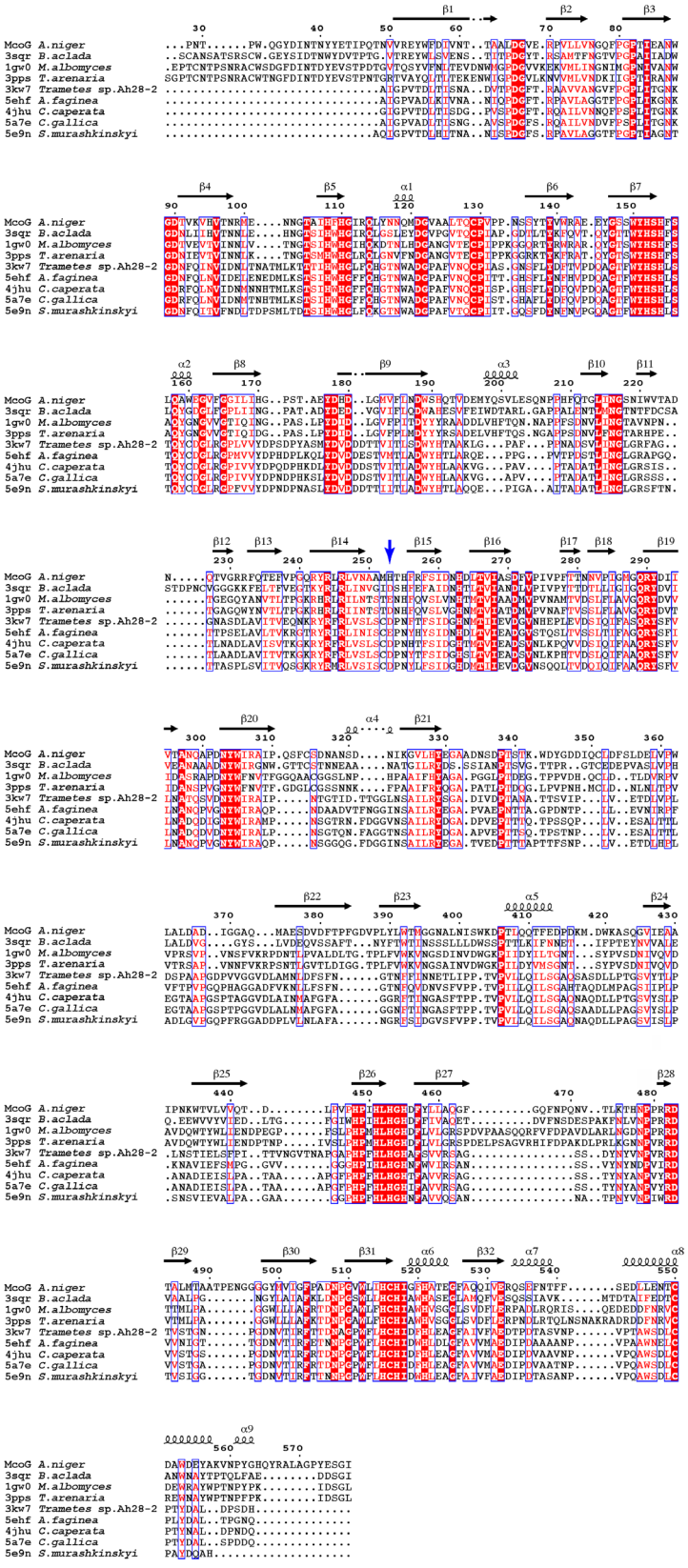

Figure 1. Alignment of the amino acid sequences for McoG from *Aspergillus niger* (5LM8) and for the laccases from *Botrytis aclada* (3SQR), *Melanocarpus albomyces* (*Ma*L, 1GW0), *Thielavia arenaria* (*Ta*L, 3PPS), *Trametes* sp. AH28-2 (3KW7), *Antrodiella faginea* (5EHF), *Coriolopsis caperata* (4JHU), *Coriolopsis gallica* (5A7E) and *Steccherinum murashkinskyi* (5E9N). Completely conserved residues are shaded with a red background. The position of residue 253 (*A. niger* McoG numbering) is indicated with a blue arrow.

are a factor of 10-20 higher compared to that for the other substrates, and especially H253A and H253N have a substantially higher K_M value compared to wt and H253D. The activity with the two amino-phenolic compounds is quite low for the H253A and H253N variants, which could indicate that the activation of the substrate by abstracting a proton from the OH-group is not possible in these two variants.

3.2 Electrochemical properties

McoG wt and variants H253D, H253A and H253N were adsorbed on a polycrystalline gold electrode coated with a SAM of decane-1-thiol (DT) taking advantage of the hydrophobic interaction between the DT-SAM and a nonpolar region of the proteins. The CV response consisted of a single well-defined signal arising from the quasi-reversible one-electron reduction/oxidation process of the Cu(II)/Cu(I) couple (Figure 3). The E°' values (Table 3) are independent of the potential scan rate, *v*, over the entire range studied (from 0.02 to 2 V s^{-1}). The current intensity is linearly dependent on the scan rate, as expected for a diffusionless electroactive species (Figure S2A and S2B). Repeated cycling does not affect the voltammograms from 5 to 35°C, indicating that the protein monolayer is stable. Above 35°C, the currents decrease and signal distortion occurs due to protein desorption and/or unfolding. The E°' values for McoG wt and variants are similar to those reported for the T1 center of low potential laccases immobilized within an electrochemically inert polymer coating a gold electrode surface [35] and to those of other asco-laccases [36].

The enthalpy and entropy changes of Cu(II) to Cu(I) reduction ($\Delta H°'_{rc}$ and $\Delta S°'_{rc}$, respectively) determined from variable temperature E°' measurements are listed in Table 3. The plots of E°' vs. T are shown in Figure S3. The reduction enthalpy $\Delta H°'_{rc}$ for type-1 copper centers

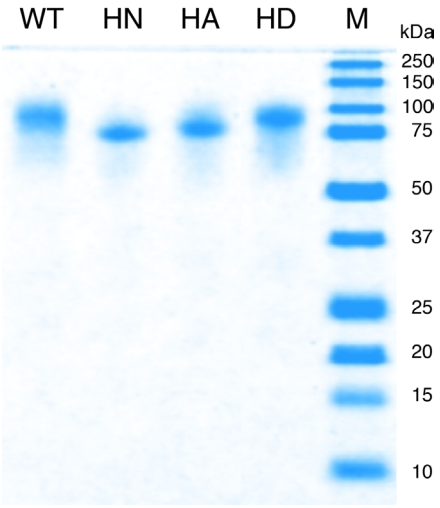

Figure 2. Tricine-SDS-PAGE gel (8%) loaded with purified samples (5 µg) of McoG wild type (WT) and variants H253D (HD), H253A (HA) and H253N (HN). Molecular masses of marker proteins (M) are indicated at the right.

in proteins is largely governed by the metal binding interactions in the ligand set. Other factors, in particular the electrostatic interactions between the solvent dipoles and the metal center, may also strongly affect its value [37, 38]. The reduction entropy is mainly affected by solvation properties of the protein, namely by reduction-induced reorganization of water molecules on the protein surface. The negative values of $\Delta S°'_{rc}$ can be related to a low exposure of the T1 center to the solvent [37, 38]. Usually, in blue copper proteins a high exposition of the metal site to the solvent is associated with high reduction entropy. $\Delta S°'_{rc}$ is positive for *Trametes versicolor* high potential laccase ($\Delta S°'_{rc}$ = +7.1 J K^{-1} mol^{-1}) [39], but negative for McoG and variants (Table 3). Within this frame, McoGs could be characterized by a relatively low exposure of the T1 site to the solvent compared to the high potential laccases or at least compared to that from *T. versicolor*. A lower degree of solvent exposure of the metal site should in principle

Table 2. Steady-state kinetic parameters of McoG wt and variants H253D, H253A H253N using DMPPDA, ABTS, 2-amino-4-methylphenol or 2-amino-4-methoxyphenol as substrates. Data are presented as the mean ± standard deviation of at least two independent experiments.

	DMPPDA*		ABTS*		2-amino-4-methylphenol#		2-amino-4-methoxyphenol#	
Enzyme	K_M **(mM)**	V_{MAX} **(U mg^{-1})**	K_M **(mM)**	V_{MAX} **(U mg^{-1})**	K_M **(mM)**	V_{MAX} **(U mg^{-1})**	K_M **(mM)**	V_{MAX} **(U mg^{-1})**
wt	1.35 ± 0.07	41 ± 0.5	15.2 ± 1.4	112.5 ± 5.4	1.43 ±0.08	80 ± 2	1.14 ± 0.09	151 ± 2
H253D	3.89 ± 0.17	50 ± 0.9	15.9 ± 1.9	114.6 ± 7.3	3.10 ± 0.09	99 ± 2	2.13 ± 0.05	129 ±2
H253A	2.43 ± 0.17	55 ± 1.3	36.7 ± 2.2	132 ± 5.4	3.22 ± 0.08	4.6± 0.2	2.66 ± 0.15	10 ± 0.6
H253N	2.95 ± 0.13	28 ± 0.4	60.4 ± 10	83 ± 11	5.50 ± 0.10	1.3 ± 0.2	4.84 ± 0.18	2.3 ± 0.1

* Determined using spectroscopy

Determined using oxygen consumption

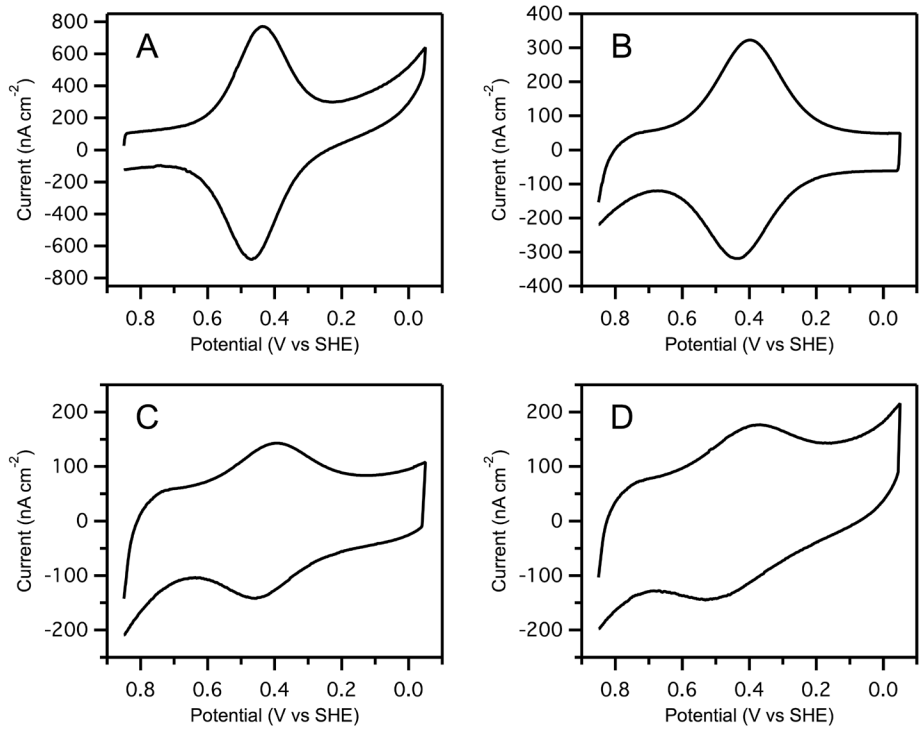

Figure 3. Cyclic voltammogram of McoG wt (A) and variants H253D (B), H253A (C), H253N (D) adsorbed on a gold electrode coated with a DT-SAM. Scan rate was 0.05 V s^{-1}, Temperature was 20°C, samples were in 20 mM Tris-Cl, 50 mM NaCl, pH 7.5.

Table 3. Thermodynamic and kinetic parameters of the reduction reaction for McoG wt and variants H253D, H253A, H253N immobilized on a polycrystalline gold electrode coated with a DT-SAM.

Protein	E°' (V)	$\Delta S°'_{rc}$ (J K^{-1} mol^{-1})	$\Delta H°'_{rc}$ (kJ mol^{-1})	k_s (s^{-1})	$\Delta H^{\#}$ (kJ mol^{-1})
McoG wt	0.453	-28	-51.9	2.4	14.4
H253D	0.417	-25	-47.5	1.8	15.2
H253A	0.426	-32	-50.6	1.1	15.9
H253N	0.448	-38	-54.4	0.4	16.4

Errors on E°', $\Delta S°'_{rc}$, and $\Delta H°'_{rc}$ are ± 0.002 V, ± 1 J K^{-1} mol^{-1} and ± 0.4 kJ mol^{-1} respectively. Errors on k_s and $\Delta H^{\#}$ are ± 6% and ± 0.4 kJ mol^{-1}, respectively.

cause stabilization of the reduced state and, hence, higher E°' value. The negative $\Delta H°'_{rc}$ values for McoG wt and variants probably arises from a strong metal ligation by the binding set in the reduced state.

The reduction potential of the H253D variant is 36 mV lower than that of the wild type protein. The enthalpic effect of this residue substitution on E°' is prominent and is that expected for the introduction of one negative charge near the metal center, namely, a more positive $\Delta H°_{rc}$ because of the preferential stabilization of the cuprous state. Conversely, the change of the entropic term is negligible. Analogous results have been obtained on a number of plastocyanin mutants subject to charge alterations on residues in the vicinity of the copper center [40]. Hence, the enthalpic effects of these mutations can be straightforwardly interpreted on simple electrostatic grounds. E°' shifts to lower values for the other variants also, but in a much more limited extent. In these cases, however, the entropic contribution to the E°' changes is remarkable or even prominent. This fact suggests that for H253A and H253N variants, the change in E°' is prevalently driven by reorganization of the solvent sphere.

The rate constants for the electron transfer process between the adsorbed proteins and the electrode, k_s

(Table 3), were determined from the scan rate dependence of the anodic and cathodic peak potentials, following the Laviron's model for diffusionless electrochemical systems [23]. Table 3 also lists the activation enthalpies ($\Delta H^{\#}$), which were calculated, using the Arrhenius equation (3),

$$k_s = A' \exp\left(\frac{-\Delta H^{\#}}{RT}\right) \quad (3)$$

from the slope of the line of a plot of $\ln(k_s)$ against 1/T (Figure S4). The values of k_s for the variants are invariably lower than for wt species, accordingly the corresponding $\Delta H^{\#}$ values are higher [41].

The redox potentials of the variants are somewhat lower for H253D and H253A compared to that of McoG wt, although with some substrates higher turnover numbers are found with these variants. For the H253N variant, an almost identical redox potential is observed as for wt, but its activity is generally quite low, which is in agreement with its low k_s value. These findings indicate that the redox potential is not the sole causes for differences in catalytic activity, but that the change in solvents sphere or in H-bonding network in the proximity of the metals center, the binding strength of substrate to the protein and its distance and orientation towards the T1-copper, are also important.

3.3 Structural properties

The crystal structure of McoG was solved using two different crystal forms at 2.65 Å (crystal form I) and 1.70 Å (crystal form II). The asymmetric unit, in both crystal forms, contains one molecule of enzyme. The crystal structure obtained from crystal form I (in the presence of zinc ions) consists of 550 amino acid residues (the first 20 amino acid residues are not visible), four copper ions, eight zinc ions, one chloride ion, eleven glucosides, one oxygen molecule, one acetate, one glycerol and 218 solvent molecules. The crystal structure obtained from crystal form II consists of 549 amino acid residues (the first 21 amino acid residues are not visible), four copper ions, fourteen glucosides, one peroxide molecule and 599 solvent molecules. The two models are very similar and their overall structure is similar to that of other laccases, especially to those from the ascomycetes *Melanocarpus albomyces* (*Ma*L) [36] and *Thielavia arenaria* (*Ta*L) (Figure 4A) [42]. The least square superposition of the Cα atoms of the McoG structure (crystal form I) with those of *Ma*L and *Ta*L gave an rmsd of 1.41 and 1.48 Å, respectively. McoG exhibits a molecular architecture organized in three sequentially arranged cupredoxin-like domains; each of them having a greek key β-barrel topology, strictly related to the small copper proteins azurin and plastocyanin and common to all members of the blue multicopper oxidase family, like ascorbate oxidase and mammalian

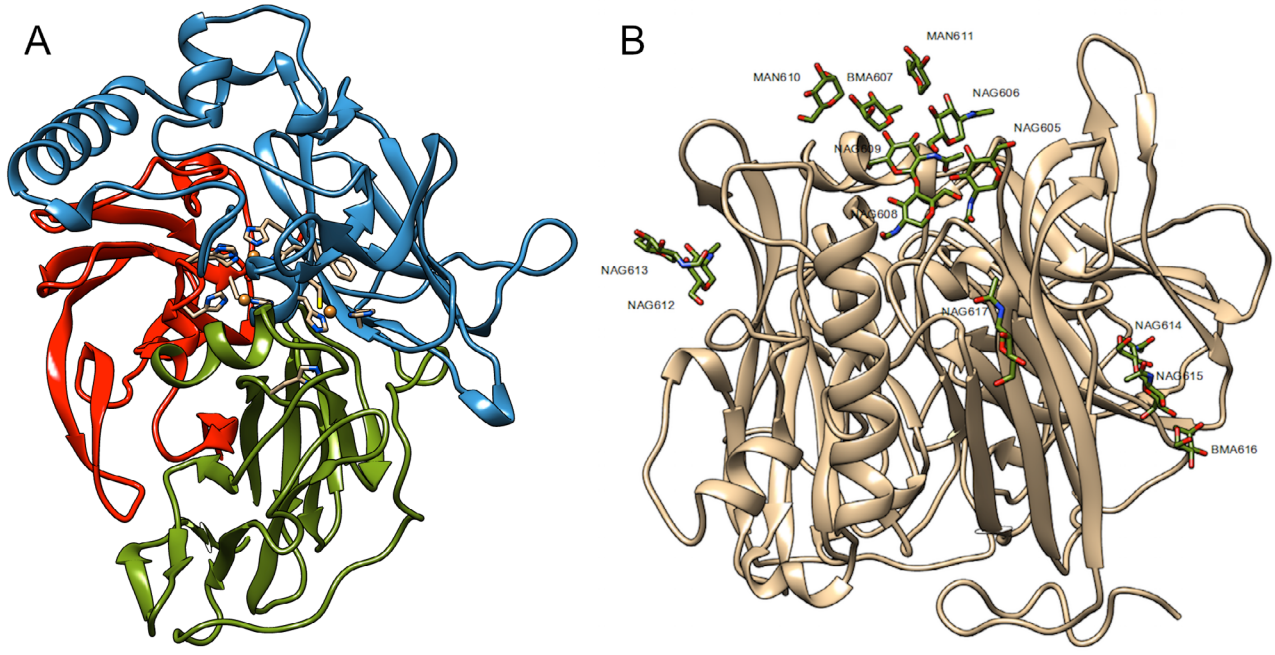

Figure 4. Ribbon diagrams of the crystal structure of wt-McoG (PDB code 5LM8). (A) illustrates the copper-binding sites (gold) and the three cupredoxin-like domains (domain A, red, domain B, green, domain C, blue). (B) highlights the glycosylation sites (carbohydrates are labeled according to the numeration in PDB with code 5LM8).

ceruloplasmin. In McoG, two disulfide bridges located in domain B (Cys314–Cys351) and between domains A and C (Cys129–Cys550) stabilize the fold. In one of the other asco-laccases with known structure an additional disulfide bridge is present near the N-terminus (Cys5-Cys13 in *Ta*L). Of the eight putative *N*-glycosylation sites with consensus sequence N-X-T/S (Asn23, Asn60, Asn103, Asn134, Asn216, Asn226, Asn400 and Asn471) only five (Asn60, Asn103, Asn134, Asn216 and Asn400) are glycosylated. The corresponding electronic densities were modeled (crystal form II) as a di(*N*-acetyl-D-glucosamine) and one mannose (Asn216), one di(*N*-acetyl-D-glucosamine) and four mannoses (Asn103), one di(*N*-acetyl-D-glucosamine) (Asn60, Asn400) and one *N*-acetyl-D-glucosamine (Asn134) (Figure 4B). Based on the electron density maps, more mannose moieties might be attached to Asn103, but the electron density was too weak to allow for the identification of the carbohydrates.

3.4 Trinuclear cluster

The trinuclear center is arranged in a similar way as is generally reported for laccases. It is composed of two type 3 coppers, each being coordinated to three His residues, and one type 2 copper coordinated to two His residues and a water molecule. In the case of the form II McoG structure the electron density maps revealed the presence of a dioxygen moiety between the two copper T3 ions. The density was more extended than the one that could be attributed to a monoatomic oxygen species and it was also slightly elliptical and tilted.

The addition of a single water molecule at this position resulted in residual electron density in the (Fo-Fc) electron-density map. Furthermore, the distances between the copper ions inside the trinuclear cluster (Table S1) are indicative of a reduction of the metal ions induced by the electrons liberated during the X-ray data collection at a synchrotron radiation source as already reported for other laccase structures [42-46]. We therefore refined a peroxide ion in this position. The O–O distance refined to 1.43 Å, without applying any restraints, consistent with the presence of a peroxide ion bridging the two T3 copper ions in the form II McoG structure (Figure 5).

A structure of an adduct with exogenous peroxide has been previously obtained with CotA, a bacterial laccase from *B. subtilis* [47] which shows the peroxide asymmetrically bound between the two T3 copper ions in an end-on bridging μ-η1:η1 mode. Also in the crystal structure of *L. tigrinus* laccase and in the structure of the untreated *B. subtilis* CotA laccase M502F mutant [44, 48] a similar peroxide adduct was observed where the peroxide ion was generated by two-electron dioxygen radiolytic reduction. A water molecule was modeled in between the two T3 copper ions in the trinuclear center of the form I McoG structure.

In laccases, two solvent channels, giving access to the trinuclear centre, were identified: a broad channel on one side of the trinuclear cluster, directed towards the T3

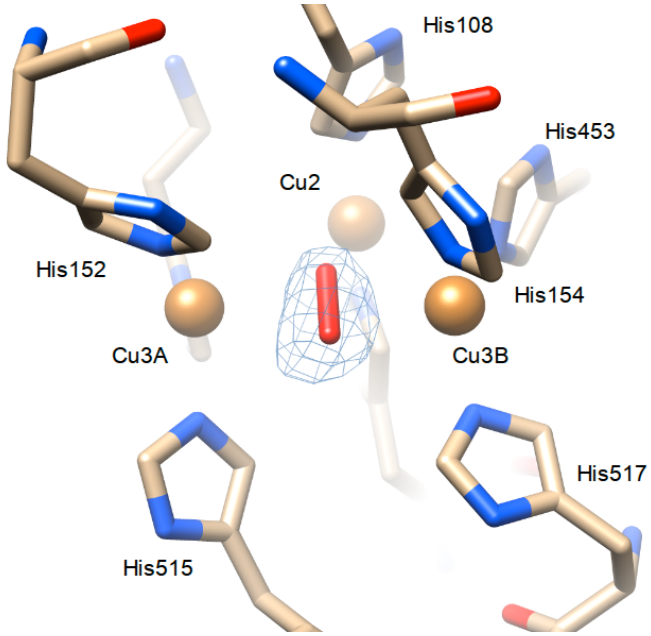

Figure 5. Trinuclear center of the McoG structure (crystal form II) showing ligandation by histidine residues and the peroxide ion bridging T3 copper atoms Cu3A and Cu3B.

Cu pair and a narrower channel on the other side of the cluster connecting the T2 Cu ion to the protein surface. In the McoG structure as in the *Ta*L structure, an arginine residue is present inside the T2 solvent channel, oriented in such a way that access to the T2 Cu ion is possible. In contrast, in *Ma*L, a histidine residue is present at that position, blocking the opening to the channel. In the asco-laccases *Ma*L and *Ta*L, the T3 channel is obstructed by their C-terminal tail. In McoG, the C-terminal tail, composed of residues ESGI (DSGL in *Ta*L and *Ma*L), penetrates also inside this channel. The C-terminus of the mature asco-laccases is highly conserved, suggesting that it is a characteristic feature of these enzymes. The role of the C-terminus in asco-laccases has not yet been clarified, even though it seems to be critical for their function. In fact, it has been reported that mutation of the last residue of *Ma*L (Leu559Ala) affects both the activity and stability of the enzyme [49] and that deletion of the four last residues resulted in an inactive form of the enzyme [50]. It has also been postulated that the C-terminal carboxylate group could assist the proton transfer for reducing the molecular oxygen, playing an analogous role as Glu498 in CotA laccase and a conserved Asp located near to the T3 coppers in basidiomyceteous laccases (Asp456 in *Trametes versicolor* laccase).

3.5 Cu T1 site

In the T1 site, copper is coordinated to the ND1 atoms of His521 and His448 and to the thiolate group of Cys516. Two other residues, Ile519 and Phe527, surround the copper T1 in an axial position at a distance (average between the two structures) of 3.3 Å and 3.6 Å, respectively. In the McoG structures several new features are visible at the T1 site. The most interesting appears the presence of a histidine (His253) (Figure 6), substituting a carboxylate residue present in all the structures of basidiomycetous laccases (Asp) [51] and in the ascomyceteous laccases from *T. arenaria* (*Ta*L, Asp236) and *M. albomyces* (*Ma*L, Glu235) [36-42] (Figure 1). The conserved Asp/Glu residue is situated close to one of the histidines that coordinates the copper T1 (His521 in McoG), in a position that allows it to interact with substrates upon their binding inside the enzyme cavity, as it has been demonstrated by the few available structures of laccase complexes with substrates or inhibitors (the structure of the complex of *Trametes versicolor* laccase with 2,5-xylidine, the structure of the complex of *Trametes trogii* laccase with 4-methylbenzoate and the structure of the complex of *Ma*L with 2,6-dimethoxyphenol) [34, 51, 52]. This carboxylate residue constitutes the only hydrophilic residue present in the highly hydrophobic substrate binding pocket of laccases and it has been reported to play a key role during the oxidation of phenolic substrates, by abstraction of a proton from the OH group [34]. The McoG structure is the first of a fungal laccase structure, which exhibits a histidine instead of a carboxylate residue in this location. However, in the bacterial laccase CotA from *Bacillus subtilis* this residue is equivalent to a threonine (Thr260) [53].

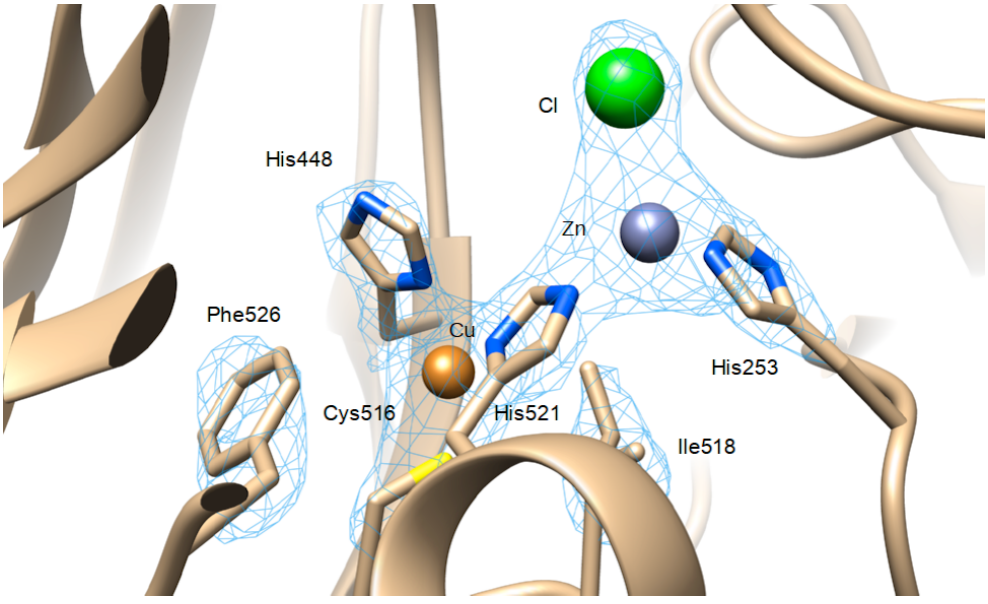

Figure 6. Copper T1 site in the McoG structure (crystal form I) with a zinc ion bound to His253 and His521. A partial (2Fo-Fc) electron-density map is shown, contoured at 1.0 σ level.

The surface charge distributions around the T1 sites of McoG, *Ta*L and *Ma*L are shown in Figure 7. The McoG charge distribution is much more negative around His253 compared to that around the Asp236 and Glu235 of the other enzymes, and possibly explains the almost absent activity of McoG with phenolic acids.

The structure of the variant H253D was solved in the monoclinic crystal form. The change from histidine to aspartate is clearly visible in the electron density maps (Figure 8A and 8B). The structure is very similar to that of the wild-type McoG structure. In the trinuclear cluster, a peroxide ion bridging the two T3 copper ions, was modeled. The aspartate side chain of residue 253, substituting the histidine, has a similar conformation in respect to the corresponding aspartate in the laccase from *T. arenaria*. The carboxylate plane of the aspartate is perpendicular to the aromatic ring of the His253 in McoG wt. The carboxylate forms hydrogen bonds with two water molecules connected to an extended solvent network, which has a different structure with respect to the McoG wt structure.

A Zn(II) ion bound to this histidine and to His521 was found in the McoG structure obtained from crystal form I. The occurrence of Zn(II) ions in the structure is due to the crystallization buffer which contained 0.2 mM zinc acetate (see Materials and Methods). His521 is one of the copper T1 ion ligands, which thus bridges both metal ions, the copper T1 and the exogenous zinc. A chloride ion and a water molecule complete the tetrahedral coordination sphere of the zinc ion (Figure 6). As already mentioned in the Materials and Methods section, several zinc ions were added to the McoG model (crystal form I), based on the electron density. Besides the zinc bound to the additional histidine (His253) located in the substrate binding site, six other zinc ions were bound at the enzyme surface. The Zn(II) ion, ligated to His 253 and His521, is located inside the substrate binding site in a position close, for example, to the position occupied by the nitrogen atom of 2,5-xylidine in the structure of the complex with *T. versicolor* laccase [51]. To our knowledge, the presence of additional metal ions in multicopper oxidases has been

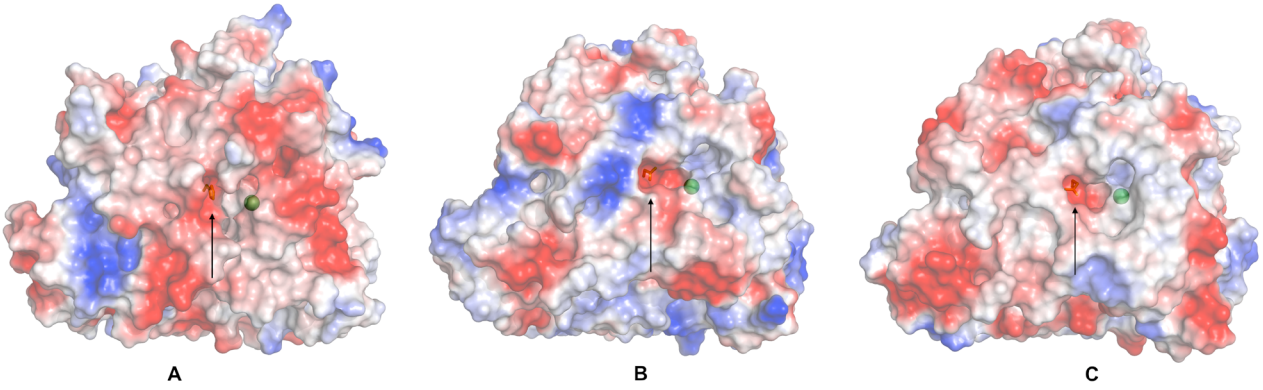

Figure 7. Surface charge distribution of McoG (A), *Ta*L (B) and *Ma*L (C); blue, positively charged regions; red, negatively charged regions. His253, Asp236 and Glu235 of these laccases, respectively, are indicated with an arrow.

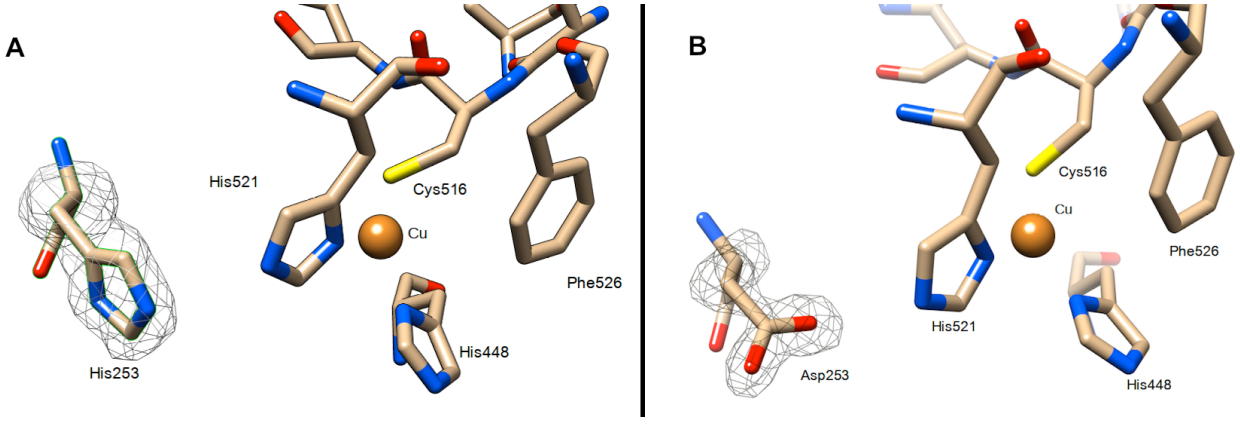

Figure 8. Copper T1 site in the McoG structure (crystal form I) showing (A), the position of His253 in McoG wt (5LM8) and (B), Asp253 in the H253D variant (5LWX). In both images, a (Fo-Fc) electron-density map is shown around His253 or Asp253, respectively, contoured at 2.5 σ level.

reported only for CueO, involved in the copper regulatory system of *E. coli* [54], which showed an enhanced oxidase activity in presence of copper. Indeed, a fifth Cu ion, close to the T1 copper site in a region rich in methionine residues, was reported for the structure of CueO soaked with $CuCl_2$ [54]. A regulatory role was suggested for the labile copper that could mediate electron transfer from the substrate to copper T1, accelerating the oxidation rate. However, measurements with or without additional Zn^{2+} or Cu^{2+} in the enzyme activity assay using McoG wt showed no difference in catalytic activity, indicating that McoG is not affected by these ions.

4 Conclusions

McoG contains near its T1 site an unusual histidine residue (His253) in a position that allows it to interact with substrates upon their binding inside the enzyme cavity. The McoG structure was solved in two crystal forms at 2.65 Å (I) and 1.7 Å (II) resolution, respectively, and in crystal form II, a peroxide ion bridge is present between the two T3 copper atoms. The conserved C-terminal tail of McoG blocks the T3 solvent channel, which is a characteristic feature of asco-laccases. We investigated the impact of the presence of His253 by replacing it with an aspartate, alanine or asparagine residue. The crystal structure of the H253D variant solved at 1.5 Å resolution shows no alteration in overall structure compared to wild type. McoG wt and the tested variants have similar activities with ABTS and DMPPDA, but their activities with 2-amino-4-methylphenol and 2-amino-4-methoxyphenol vary considerably. The low redox potential determined for McoG wt is comparable to other asco-laccases. The electron transfer rates (k_s) of wt and variants were determined, and especially the reduced k_s values of H253N and H253A showed strong correlation with their low activity on phenolic compounds. In summary, McoG has adapted a histidine at position 253 instead of the common aspartate or glutamate, and our results show that this adaptation can be beneficial for the conversion of phenolic compounds, especially as asco-laccases are used in biosensors for on-line and *in situ* monitoring of this type of molecules.

Acknowledgements: We thank Ian de Bus for performing McoG activity measurements and Tom Schonewille for assistance with *A. niger* culturing. One data collection was performed on beamline ID29 at the ESRF, Grenoble, France. We are grateful to Local Contact at the ESRF for providing assistance in using beamline ID29. We thank the ALBA staff at ALBA Synchrotron facility for providing assistance in data collection on the XALOC beamline used for the other experiments.

Competing interests: The authors declare that they have no competing interests.

References

[1] Hoegger, P.J., Kilaru, S., James, T.Y., Thacker, J.R. & Kües, U., Phylogenetic comparison and classification of laccase and related multicopper oxidase protein sequences, FEBS J., 2006, 273, 2308-2326.

[2] Sakurai, T. & Kataoka, K., Basic and applied features of multicopper oxidases, CueO, bilirubin oxidase, and laccase, Chem. Rec., 2007, 7, 220-229.

[3] Quintanar, L., Stoj, C., Taylor, A.B., Hart, P.J., Kosman, D.J. & Solomon, E.I., Shall we dance? How a multicopper oxidase chooses its electron transfer partner, Acc. Chem. Res., 2007, 40, 445-452.

[4] Giardina, P., Faraco, V., Pezzella, C., Piscitelli, A., Vanhulle, S. & Sannia, G., Laccases: a never-ending story, Cell. Mol. Life Sci., 2010, 67, 369-385.

[5] Baldrian, P., Fungal laccases - occurrence and properties, FEMS Microbiol. Rev., 2006, 30, 215-242.

[6] Schouten, A., Wagemakers, L., Stefanato, F.L., van der Kaaij, R.M. & van Kan, J.A., Resveratrol acts as a natural profungicide and induces self-intoxication by a specific laccase, Mol. Microbiol., 2002, 43, 883-894.

[7] Maté, D., García-Ruiz, E., Camarero, S. & Alcalde, M., Directed evolution of fungal laccases, Curr. Genomics, 2011, 12, 113-122.

[8] Shraddha, Shekher, R., Sehgal, S., Kamthania, M. & Kumar, A., Laccase: microbial sources, production, purification, and potential biotechnological applications, Enzyme Res., 2011, 2011, 2011:217861.

[9] Tetsch, L., Bend, J. & Hölker, U., Molecular and enzymatic characterisation of extra- and intracellular laccases from the acidophilic ascomycete *Hortaea acidophila*, Anton. Leeuw., 2006, 90, 183-194.

[10] Tamayo-Ramos, J.A., Barends, S., Verhaert, R.M.D. & de Graaff, L.H., The *Aspergillus niger* multicopper oxidase family: analysis and overexpression of laccase-like encoding genes, Microb. Cell. Fact., 2011, 10, 78.

[11] Hoshida, H., Nakao, M., Kanazawa, H., Kubo, K., Hakukawa, T., Morimasa, K., Akada, R. & Nishizawa, Y., Isolation of five laccase gene sequences from the white-rot fungus *Trametes sanguinea* by PCR, and cloning, characterization and expression of the laccase cDNA in yeasts, J. Biosci. Bioeng., 2001, 92, 372-380.

[12] Cordoba Cañero, D.C. & Roncero, M.I.G., Functional analyses of laccase genes from *Fusarium oxysporum*, Phytopathology, 2008, 98, 509-518.

[13] Courty, P.E., Hoegger, P.J., Kilaru, S., Kohler, A., Buée, M., Garbaye, J., Martin, F. & Kües, U., Phylogenetic analysis, genomic organization, and expression analysis of multi-copper oxidases in the ectomycorrhizal basidiomycete *Laccaria bicolor*, New Phytol., 2009, 182, 736-750.

[14] Mander, G.J., Wang, H., Bodie, E., Wagner, J., Vienken, K., Vinuesa, C., Foster, C., Leeder, A.C., Allen, G., Hamill, V., et al., Use of laccase as a novel, versatile reporter system in filamentous fungi, Appl. Environ. Microbiol., 2006, 72, 5020-5026.
[15] Tamayo-Ramos, J.A., van Berkel, W.J.H. & de Graaff, L.H., Biocatalytic potential of laccase-like multicopper oxidases from *Aspergillus niger*, Microb. Cell. Fact., 2012, 11.
[16] Sambrook, J., Fritsch, E.F. & Maniatis, T., Molecular cloning: a laboratory manual, 2nd ed., Cold Spring Harbor Laboratory Press, Cold Spring Harbor, N.Y. , 1989.
[17] de Graaff, L.H., van den Broek, H. & Visser, J., Isolation and transformation of the pyruvate kinase gene of *Aspergillus nidulans*, Cur. Genetics., 1988, 13, 315-321.
[18] Oliveira, J.M., van der Veen, D., de Graaff, L.H. & Qin, L., Efficient cloning system for construction of gene silencing vectors in *Aspergillus niger*, Appl. Microbiol. Biotechnol., 2008, 80, 917-924.
[19] Pei, J., Bong-Hyun, K., B-H. & Grishin, N.V., PROMALS3D: a tool for multiple sequence and structure alignment, Nucl. Acids Res., 2008, 36, 2295-2300.
[20] Robert, X. & Gouet, P., Deciphering key features in protein structures with the new ENDscript server, Nucl. Acids Res., 2014, 42, W320-W324.
[21] Pontecorvo, G., Roper, J.A., Chemmons, L.M., Macdonald, K.D. & Bufton, A.W.J., The genetics of *Aspergillus nidulans*, Adv. Genet., 1953, 5, 141-238.
[22] van der Veen, D., Oliveira, J.M., van den Berg, W.A.M. & de Graaff, L.H., Analysis of variance components reveals the contribution of sample processing to transcript variation, Appl. Environ. Microbiol., 2009, 75, 2414-2422.
[23] Laviron, E., General expression of the linear potential sweep voltammogram in the case of diffusionless electrochemical systems, J. Electroanal. Chem. Interfacial Electrochem., 1979, 101, 19-28.
[24] Yee, E.L., Cave, R.J., Guyer, K.L., Tyma, P.D. & Weaver, M.J., A survey of ligand effects upon the reaction entropies of some transition metal redox couples, J. Am. Chem. Soc., 1979, 101, 1131-1137.
[25] Yee, E.L. & Weaver, M.J., Functional dependence upon ligand composition of the reaction entropies for some transition-metal redox couples containing mixed ligands, Inorg. Chem., 1980, 19, 1077-1079.
[26] Taniguchi, V.T., Sailasuta-Scott, N., Anson, F.C. & Gray, H.B., Thermodynamics of metalloprotein electron transfer reactions, Pure Appl. Chem., 1980, 52, 2275-2281.
[27] Kabsch, W., Integration, scaling, space-group assignment and post-refinement, Acta Crystallogr. D: Biol. Crystallogr., 2010, 66(Pt 2), 133-144.
[28] Vagin, A.A. & Teplyakov, A., MOLREP: an automated program for molecular replacement, J. Appl. Cryst., 1997, 30, 1022-1025.
[29] Murshudov, G.N., Vagin, A.A. & Dodson, E.J., Refinement of macromolecular structures by the Maximum-Likelihood method, Acta Crystallogr. D: Struc. Biol., 1997, 53, 240-255.
[30] Emsley, P., Lohkamp, B., Scott, W.G. & Cowtan, K., Features and development of Coot, Acta Crystallogr. D: Biol. Crystallogr., 2010, 66(Pt 4), 486-501.
[31] Lamzin, V.S., Perrakis, A. & Wilson, K.S. ARP/wARP – automated model building and refinement in *International Tables for Crystallography* 720-722, Kluwer Academic Publishers, Dordrecht, The Netherlands (2001).
[32] Lovell, S.C., Davis, I.W., Arendall III, W.B., de Bakker, P.I., Word, J.M., Prisant, M.G., Richardson, J.S. & Richardson, D.C., Structure validation by Calpha geometry: phi,psi and Cbeta deviation, Proteins, 2003, 15, 437-450.
[33] Rodríguez-Delgado, M.M., Alemán-Nava, G.S., Rodríguez-Delgado, J.M., Dieck-Assad, G., Martínez-Chapa, S.O., Barceló, D. & Parra, R., Laccase-based biosensors for detection of phenolic compounds, TRAC, 2015, 74, 21-45.
[34] Kallio, J.P., Auer, S., Jänis, J., Andberg, M., Kruus, K., Rouvinen, J., Koivula, A. & Hakulinen, N., Structure-function studies of a *Melanocarpus albomyces* laccase suggest a pathway for oxidation of phenolic compounds, J. Mol. Biol., 2009, 392, 895-909.
[35] Frasconi, M., Favero, G., Boer, H., Koivula, A. & Mazzei, F., Kinetic and biochemical properties of high and low redox potential laccases from fungal and plant origin, Biochim. Biophys. Acta, 2010, 1804, 899-909.
[36] Kallio, J.P., Gasparetti, C., Andberg, M., Boer, H., Koivula, A., Kruus, K., Rouvinen, J. & Hakulinen, N., Crystal structure of an ascomycete fungal laccase from *Thielavia arenaria* - common structural features of asco-laccases, FEBS J., 2011, 278, 2283-2295.
[37] Battistuzzi, G., Borsari, M., Sola, M. & Francia, F., Redox thermodynamics of the native and alkaline forms of eukaryotic and bacterial class I cytochromes c, Biochemistry, 1997, 36, 16247-16258.
[38] Battistuzzi, G., Borsari, M., Loschi, L., Martinelli, A. & Sola, M., Thermodynamics of the alkaline transition of cytochrome c, Biochemistry, 1999, 38, 7900-7907.
[39] Taniguchi, V.T., Malmström, B.G., Anson, F.C. & Gray, H.B., Temperature dependence of the reduction potential of blue copper in fungal laccase, Proc. Natl. Acad. Sci. USA, 1982, 79, 3387-3389.
[40] Battistuzzi, G., Borsari, M., Loschi, L., Menziani, M.C., De Rienzo, F. & Sola, M., Control of metalloprotein reduction potential: the role of electrostatic and solvation effects probed on plastocyanin mutants, Biochemistry, 2001, 40, 6422-6430.
[41] Warren, J.J., Lancaster, K.L., Richards, J.H. & Gray, H.B., Inner- and outer-sphere metal coordination in blue copper proteins, J. Inorg. Biochem., 2012, 115, 119-126.
[42] Hakulinen, N., Kiiskinen, L.L., Kruus, K., Saloheimo, M., Paananen, A., Koivula, A. & Rouvinen, J., Crystal structure of a laccase from *Melanocarpus albomyces* with an intact trinuclear copper site, Nat. Struct. Biol., 2002, 9, 601-605.
[43] Ferraroni, M., Matera, I., Chernykh, A., Kolomytseva, M., Golovleva, L.A., Scozzafava, A. & Briganti, F., Reaction intermediates and redox state changes in a blue laccase from *Steccherinum ochraceum* observed by crystallographic high/low X-ray dose experiments, J. Inorg. Bioch., 2012, 111, 203-209.
[44] Ferraroni, M., Myasoedova, N.M., Schmatchenko, V., Leontievsky, A.A., Golovleva, L.A., Scozzafava, A. & Briganti, F., Crystal structure of a blue laccase from *Lentinus tigrinus*: Evidences for intermediates in the molecular oxygen reductive splitting by multicopper oxidases, BMC Struct. Biol., 2007, 7, 60.
[45] Garavaglia, S., Cambria, M.T., Miglio, M., Ragusa, S., Iacobazzi, V., Palmieri, F., D'Ambrosio, C., Scaloni, A. & Rizzi,

M., The structure of *Rigidoporus lignosus* Laccase containing a full complement of copper ions, reveals an asymmetrical arrangement for the T3 copper pair, J. Mol. Biol., 2004, 342, 1519-1531.
[46] Komori, H., Sugiyama, R., Kataoka, K., Miyazaki, K., Higuchi, Y. & Sakurai, T., New insights into the catalytic active-site structure of multicopper oxidases, Acta Crystallogr. D: Biol. Crystallogr., 2014, D70, 772-779.
[47] Bento, I., Martins, L.O., Gato Lopes, G., Arménia Carrondo, M. & Lindley, P.F., Dioxygen reduction by multi-copper oxidases; a structural perspective, Dalton Trans., 2005, 21, 3507-3513.
[48] Durão, P., Bento, I., Fernandes, A.T., Melo, E.P., Lindley, P.F. & Martins, L.O., Perturbations of the T1 copper site in the CotA laccase from *Bacillus subtilis*: structural, biochemical, enzymatic and stability studies, J. Biol. Inorg. Chem., 2006, 11, 514-526.
[49] Andberg, M., Hakulinen, N., Auer, S., Saloheimo, M., Koivula, A., Rouvinen, J. & Kruus, K., Essential role of the C-terminus in *Melanocarpus albomyces* laccase for enzyme production, catalytic properties and structure, FEBS J., 2009, 276, 6285-6300.
[50] Zumárraga, M., Camarero, S., Shleev, S., Martínez-Arias, A., Ballesteros, A., Plou, F.J. & Alcalde, M., Altering the laccase functionality by in vivo assembly of mutant libraries with different mutational spectra, Proteins, 2008, 71, 250-260.
[51] Bertrand, T., Jolivalt, C., Briozzo, P., Caminade, E., Joly, N., Madzak, C. & Mougin, C., Crystal structure of a four-copper laccase complexed with an arylamine: insights into substrate recognition and correlation with kinetics, Biochemistry, 2002, 41, 7325-7333.
[52] Matera, I., Gullotto, A., Tilli, I., Ferraroni, M., Scozzafava, A. & Briganti, F., Crystal structure of the blue multicopper oxidase from the white-rot fungus *Trametes trogii* complexed with *p*-toluate, Inorg. Chim. Acta, 2008, 361, 4129-4137.
[53] Enguita, F. J., Marçal, D., Martins, L.O., Grenha, R., Henriques, A.O., Lindley, P.F., Carrondo, M.A., Substrate and dioxygen binding to the endospore coat laccase from *Bacillus subtilis*. J. Biol. Chem., 2004, 279, 23472-23476.
[54] Roberts, S.A., Wildner, G.F., Grass, G., Weichsel, A., Ambrus, A., Rensing, C. & Montfort, W.R., A labile regulatory copper ion lies near the T1 copper site in the multicopper oxidase CueO, J. Biol. Chem., 2003, 278, 31958-31963.

Supplemental Material: The online version of this article (DOI: 10.1515/boca-2017-0001) offers supplementary material.

Supplementary Material to:

Structure and function of *Aspergillus niger* laccase McoG

Marta Ferraroni, Adrie H. Westphal, Marco Borsari, Juan Antonio Tamayo-Ramos, Fabrizio Briganti, Leo H. de Graaff, and Willem J. H. van Berkel

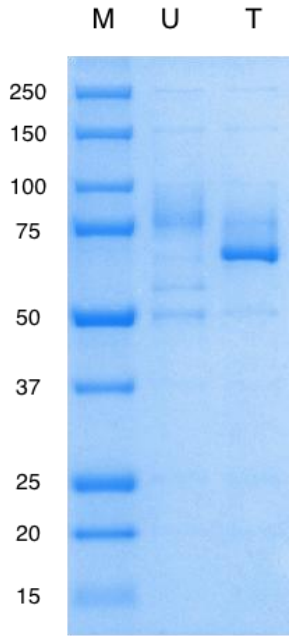

Fig S1. SDS-PAGE gel (10%) loaded with purified wild-type McoG (U) and purified wild-type McoG after treatment with endoglycosidase H (T). Molecular masses of marker proteins (M) are indicated at the left. Minor amounts of marker bands are also visible in the U and T lanes.

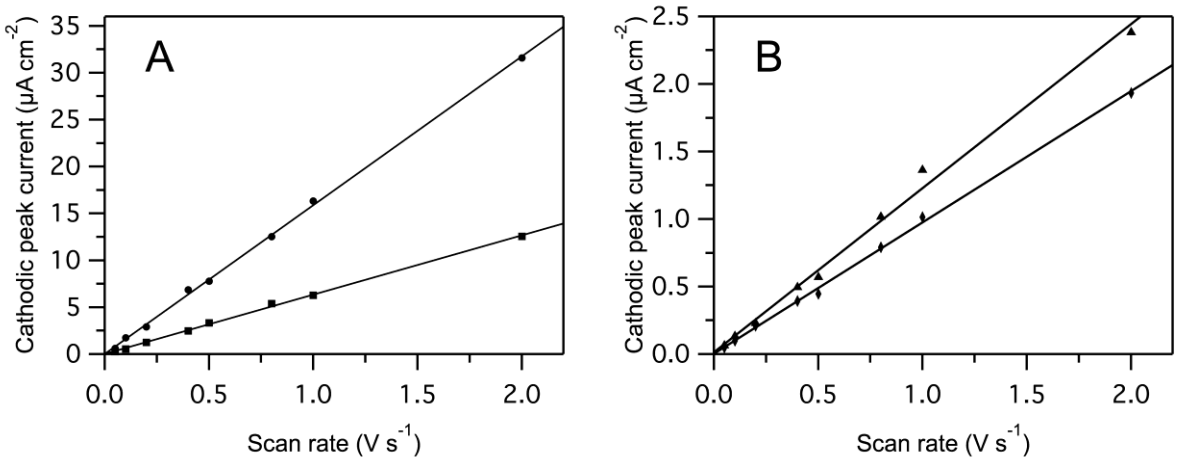

Figure S2. Cathodic peak current (μA cm^{-2}) vs. scan rate (V s^{-1}) plot for McoG wt and variants adsorbed on a gold electrode coated with a DT-SAM. A: McoG wt, spheres; H253D, squares; B: H253A, triangles, H253N, diamonds. Temperature was 5°C, samples were in 20 mM Tris-Cl, 50 mM NaCl, pH 7.5. R^2-values obtained after least square fitting the data to the equation Y=a+b*X are 0.9990, 0.9987, 0.9936 and 0.9986 for McoG wt, H253D, H253A and H253N, respectively.

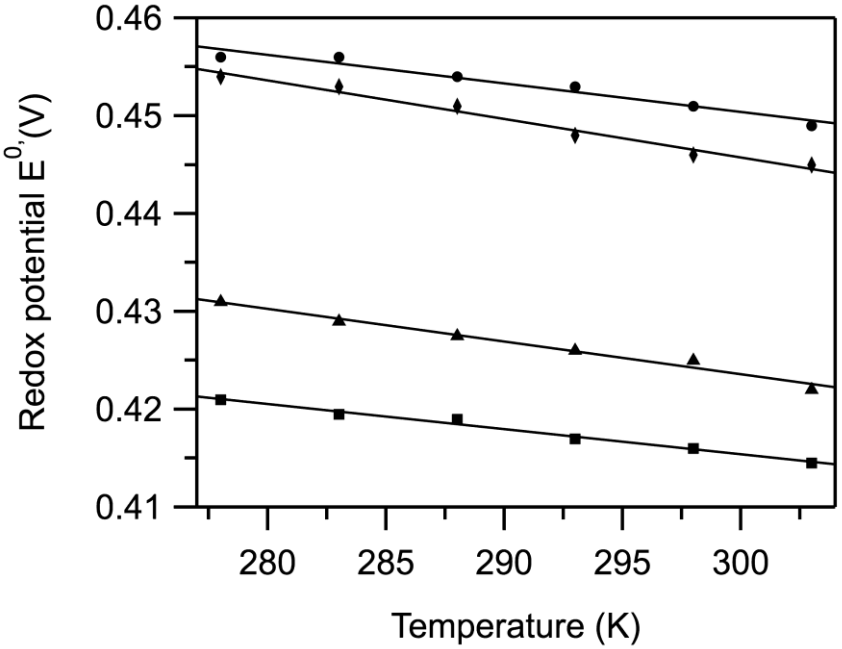

Figure S3. Redox potential (E°') vs. temperature (T) plot of McoG wt and variants adsorbed on gold DT-SAM modified electrode. Scan rate was 0.05 V s^{-1}. Spheres, McoG wt; squares, H253D; triangles, H253A; diamonds, H253N. Samples were in 20 mM Tris-Cl, 50 mM NaCl, pH 7.5. R^2-values obtained after least square fitting the data to the equation Y=a+b*X are 0.9568, 0.9862, 0.9802 and 0.9786 for McoG wt, H253D, H253A and H253N, respectively.

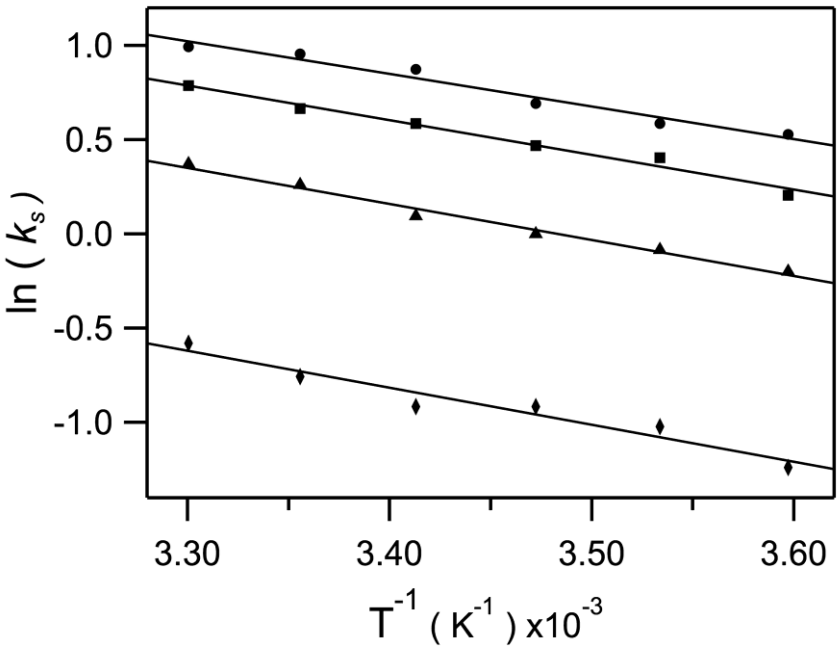

Figure S4. ln (k_s) vs. 1/T plots (Arhenius plot) of McoG wt and variants adsorbed on a gold electrode coated with a DT-SAM. Spheres, McoG wt; squares, H253D; triangles, H253A; diamonds, H253N. Samples were in 20 mM Tris-Cl, 50 mM NaCl, pH 7.5. R^2-values obtained after least square fitting the data to the equation Y=a+b*X are 0.9666, 0.9822, 0.9856 and 0.9444 for McoG wt, H253D, H253A and H253N, respectively.

Table S1. Distances between copper ions in the trinuclear center in McoG. For comparison, also copper-copper distances as measured in other laccases are reported. MaL (Melanocarpus albomyces laccase), TvL (Trametes versicolor laccase) and LtL (Lentinus tigrinus laccase). Distances in MaL and LtL are typical for the reduced oxidation state of the coppers.

Copper pair	McoG (form I) (Å)	McoG (form II) (Å)	MaL (Å)	TvL (Å)	LtL (Å)
Cu3(a) - Cu3	4.4	5.0	4.9	3.91	4.9
Cu2 - Cu3(a)	3.8	3.9	3.9	3.81	4.3
Cu2 - Cu3(b)	4.1	4.0	4.2	3.82	4.1